Acta Materialia 108 (2016) 264-270

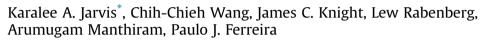
Contents lists available at ScienceDirect

Acta Materialia

journal homepage: www.elsevier.com/locate/actamat

Full length article

Formation and effect of orientation domains in layered oxide cathodes of lithium-ion batteries



Materials Science and Engineering Program & Texas Materials Institute, The University of Texas at Austin, Austin, TX 78712, USA

ARTICLE INFO

Article history: Received 1 January 2016 Received in revised form 11 February 2016 Accepted 15 February 2016

Keywords: Li-ion batteries Layered oxide cathodes Transmission electron microscopy Phase transition Nanodomains

ABSTRACT

We show that in layered oxides that are employed as cathodes in lithium-ion batteries, the cation layers can order on different $\{111\}_{NaCl}$ planes within a single particle, which makes the lithium layer discontinuous across a particle. The findings challenge previous assertions that lithium undergoes 2-D diffusion in layered oxides and the data provide new insights into the decrease in rate capabilities for some layered oxides. Therefore, it is critically important to understand how these discontinuities form and how the loss of 2-D diffusion impacts the overall performance of the layered oxide cathode materials. Employing X-ray diffraction (XRD) and aberration-corrected scanning transmission electron microscopy (STEM), we find that as the material transitions from a disordered to an ordered state, it forms four orientation variants corresponding to the four $\{111\}_{NaCl}$ planes. This transition is not intrinsic to all layered oxides and appears to be more strongly affected by nickel. Furthermore, with energy dispersive spectroscopy (EDS), we show that there is an increase in the nickel concentration at the interface between each orientation variant. This reduces the rate of lithium diffusion, negatively affects the rate capability, and could be contributing to the overall capacity fade.

Published by Elsevier Ltd on behalf of Acta Materialia Inc.

1. Introduction

With an aim to reduce the cost and improve the safety of Li-ion batteries, much focus has been directed in recent years towards novel materials composed of layered Li[Li_{1/3}Mn_{2/3}]O₂, generally designated as Li_2MnO_3 , and $LiMO_2$ [M = Mn, Ni, Co]. Among them, the Li[Li_{1/3-2x/3}Mn_{2/3-x/3}Ni_x]O_2 (0 < x \leq $^{1\!\!/_2})$ series has shown promise due to its high capacity [1–6]. We showed that compositions within the Li[Li_{1/3-2x/3}Mn_{2/3-x/3}Ni_x]O_2 (0 < x \leq $^{1\!\!/_2})$ series prepared by two different methods exhibits either an $R\overline{3}m$ phase, C_2/m phase, or both phases depending on the value of x [7]. More interestingly, we showed that regardless of composition, the cation layers in the Li[Li_{1/3-2x/3}Mn_{2/3-x/3}Ni_x]O₂ (0 < x \leq ¹/₂) series order on different {111}_{NaCl} planes in the base NaCl structure within a single particle. Initially, we will refer to areas of different ordering as domains. We also showed that particles with multiple domains are single-phase but appear to consist of multiple phases when viewed in projection [7].

http://dx.doi.org/10.1016/j.actamat.2016.02.034 1359-6454/Published by Elsevier Ltd on behalf of Acta Materialia Inc. As reported, we observed this phenomenon in four different compositions prepared with two different precursors. As we will show in this work, we see the same ordering in samples heat treated for different times and at different temperatures. In total, 14 different samples within the Li[Li_{1/3}-2x/3Mn_{2/3}-x/3Ni_x]O₂ (0 < x ≤ ½) series and over 70 different particles show changes in cation ordering, leading to an effective change in the orientation of the trigonal or monoclinic structure within the same particle. These domains result in discontinuities of the lithium layers across a single particle. Hence, particles in the Li[Li_{1/3}-2x/3Mn_{2/3}-x/3Ni_x]O₂ (0 < x ≤ ½) series can no longer be assumed to exhibit 2-D lithium diffusion, contrary to the previous assertion.

With this perspective, we focus here on how these domains forms, if they are intrinsic to all layered oxides, and how they affect the overall electrochemical properties in lithium-ion cells. Accordingly, in this paper, we examine, by aberration-corrected scanning transmission electron microscopy (STEM), two samples, LiCoO₂ and Li₂MnO₃, in addition to the Li[Li_{1/3}–2x/3Mn_{2/3}–x/3Ni_x]O₂ (0 < x \leq ½) series. We also investigate the disorder-to-order transition with X-ray diffraction (XRD) to explain the change in the ordering. Finally, we examine the rate capability of the system with and without the changes in ordering and consider the impact on





Acta MATERIALIA

^{*} Corresponding author. E-mail address: kjarvis@austin.utexas.edu (K.A. Jarvis).

capacity fade.

2. Experimental

2.1. Materials and synthesis

The Li[Li_{1/3-2x/3}Mn_{2/3-x/3}Ni_x]O₂ series was prepared with a solgel synthesis process. Required amounts of lithium acetate, manganese acetate, and nickel acetate were dissolved in deionized water. Ethylenediaminetetraacetic acid (EDTA) and citric acid, acting as complexing agents, were added to NH₄OH to form a homogeneous aqueous solution with pH ~ 8. The metal acetate solution was then added to the EDTA/citric acid solution. The mole ratio of EDTA:citric acid:metal ion was 1:1.5:1. The mixtures were then heat treated at 90 °C for 12 h until a gel was formed. This gel was then fired at 450 °C for 6 h to remove the residual organic impurities. The resulting powder was then heated at 900 °C for 12 h to obtain the final powder, unless otherwise indicated.

2.2. Characterization

XRD data were collected with a Philips X'pert diffractometer. For transmission electron microscopy (TEM) analysis, the powders were suspended in ethanol or methanol and placed on a carbon lacey grid. Images and compositional analysis were collected at The University of Texas at San Antonio, with a JEOL ARM200F TEM/ STEM, equipped with a CEOS GmbH corrector for the illuminating lenses, a high-angle annular dark-field (HAADF) detector, and an EDAX energy dispersive X-ray spectrometer. Selected area electron diffraction (SAED) and energy dispersive X-ray spectroscopy (EDS) was performed on a JEOL 2010F TEM equipped with an Oxford energy dispersive X-ray detector.

3. Results and discussion

As we showed in our previous work, a change in the ordering of the cation layers on the $\{111\}_{NaCl}$ planes occurs in samples of various compositions and prepared with different precursors and heat treated at 900 °C for 12 h [7]. We see the same trend with samples of Li[Li_{0.2}Mn_{0.6}Ni_{0.2}]O₂ heat treated at 850 °C for 24 h and heated at 900 °C for 6 h, 24 h, and 72 h (Fig. 1). In order to understand how these domains form, we must identify the type of domains and the respective boundaries.

3.1. Domain formation

For this discussion, we again use the rock-salt (NaCl)-structure for comparison because it is the basic structure for layered oxides [8] and allows us to more easily compare different compositions and their resulting phases. Fig. 2 shows the interface between two domains of different ordering for the material Li[Li_{0.067}Mn_{0.533}Ni_{0.4}] O₂, in particular, region 1 is ordered on the (111)_{NaCl} plane, while region 2 is ordered on the (111)_{NaCl} plane. The boundary between these two regions is clearly not sharp and has characteristics of both domains. In fact, the transition-metal layer of region 1 slowly changes from bright atomic columns, spaced by 1.4 Å to bright atomic columns spaced by 2.8 Å, until it reaches region 2. In addition, the interfacial region shows that the transition metals begin to occupy the lithium layer of region 1 until it fully transforms to region 2.

By initial observation, the boundary appears to be a type of highangle grain boundary. Grain boundaries form during solidification, deformation and recrystallization, or phase transformation due to macroscopic diffusion (diffusion of more than a few nearest neighbors) [9]. This material never went through solidification or deformation and macroscopic diffusion would require heterogeneous compositional variations on a large scale. Although we cannot yet rule out grain boundaries entirely, there are two boundaries that are more likely to form in these materials during disorder-order transitions. As these materials go through a disorder-to-order process, orientation variants and/or anti-phase domains can form [10,11]. The type of domain formed will depend on the starting and final structures.

In the case of our samples, which were first heated at 450 °C for 6 h to remove the organic residues, XRD shows that Li $[Li_{0.2}Mn_{0.6}Ni_{0.2}]O_2$ exhibits a spinel-like structure with an $Fd\overline{3}m$ space group, as indicated by the single broad X-ray peak near 65° (Fig. 3). These results are similar to the previous work by Lu et al. for Li[Mn_{0.5}Ni_{0.5}]O₂ synthesized at 600 °C [6]. Due to the broad nature of the peak near 65° and the peaks in the 25–35° range, which indicate lithium ordering in the transition-metal layer, some of the material may have already formed a layered structure. As we have shown in a previous work, these materials have less homogeneity at lower temperatures [12]. Therefore, we propose that this material contains some particles with spinel-like structure while others exhibit an ordered layered structure. However, after heat treatment at 900 °C, the sample has fully transitioned from the initial $Fd\overline{3}m$ space group to either an $R\overline{3}m$ or C2/m space group, depending on the composition [7]. Furthermore, *in-situ* XRD heating at 900 °C for 12 h reveals that the material is mostly layered, as indicated by the peak splitting near 64° (Fig. S1). The in-situ XRD shows a small amount of a spinel-like phase, as indicated by the shoulder on the peak at 44.2°, and an NaCl-like phase, as indicated by the small peaks around 37.5°, 43° and 62.6°; however, these could be the result of the loss of lithium during the *in-situ* XRD heating [12]. Overall, the material does not significantly disorder at 900 °C and, therefore, the disorder-to-order transition happens mostly when the material orders after the initial heat treatment.

Now that we know the starting and ending phases of the disorder-to-order transition, we can predict what type of boundaries are present between the different orientations. $R\overline{3}m$ is a "translationengleiche" subgroup of $Fd\overline{3}m$ and C2/m is a "translationengleiche" subgroup of $R\overline{3}m$ [13]. Only point group symmetry operators of the parent phase are lost during the disorder-to-order transition of "translationengleiche" subgroups [13]. Accordingly, the interfaces observed in these materials should be orientation variant boundaries, not anti-phase boundaries, which require a loss of translational symmetry [10].

To confirm that the domains are orientation variants, we must verify that each variant can transition into the other from one of the lost point group symmetry operators [10,14]. The $Fd\overline{3}m \rightarrow R\overline{3}m$ transition should produce four orientation variants as the material transitions from 48 symmetry operators to 12 symmetry operators [10,15]. This explains the changes in cation ordering occurring in four different {111}_{NaCl} planes. The lost symmetry operators of the $Fd\overline{3}m \rightarrow R\overline{3}m$ transition are the 4⁺, 4⁻, $\overline{4}^+$, $\overline{4}^-$, and d. To begin, let us first consider if any of the orientation variants can translate into one another by a fourfold axis of rotation in the clockwise direction. The three 4⁺ axes of rotation in $Fd\overline{3}m$ are on the three $<001>_{NaCl}$ zone axes [13], which correspond to the $[841]_T$, $[\overline{4}41]_T$, and $[\overline{48}1]_T$ axes in the $R\overline{3}m$ space group. Due to the overlap of different types of atoms along these zone axes, it is not possible to depict the transitions with a simple schematic. Instead, let us consider the $[210]_T$ zone axis, in which like atoms stack on top of each other (Fig. 4a). When rotated 90° clockwise about the $[841]_T$ axis, the crystal is now aligned along the [8 10 1]_T zone axis (Fig. 4b), which corresponds to configuration A₃ as defined in a previous paper (Fig. S2) [7]. Another 90° clockwise rotation about the [841]_T axis brings the crystal to the [211]_T zone axis (Fig. 4c), which corresponds to configuration A₄ [7]. The last 90° clockwise rotation produces an Download English Version:

https://daneshyari.com/en/article/7878643

Download Persian Version:

https://daneshyari.com/article/7878643

Daneshyari.com